의학석사 학위논문

Differential roles of Kv4.1 and Kv4.2 channels in excitatory postsynaptic responses in the hippocampus

해마 신경세포의 흥분성 후시냅스 반응에 대한 Kv4.1 과 Kv4.2 채널의 차별적인 역할

2017년 2월

서울대학교 대학원

의과학과 생리학 전공

권 민 정

A thesis of the Master's Degree

해마 신경세포의 흥분성 후시냅스 반응에 대한 Kv4.1 과 Kv4.2 채널의 차별적인 역할

Differential roles of Kv4.1 and Kv4.2 channels in excitatory postsynaptic responses in the hippocampus

February 2017

The Department of Physiology,
Seoul National University
College of Medicine
Min Jeong Kwon

ABSTRACT

A-type K^+ channel is important in the integration of subthreshold synaptic potentials and it is suggested that signaling mechanisms by regulation of A-type K^+ channel could profoundly influence neuronal excitability. Among the Kv4 family, the intrinsic property of Kv4.1 and Kv4.2 channels are widely studied. Until today, however, the contribution of A-type K^+ channel in synaptic plasticity remains unknown.

The effectiveness of inhibition of K^+ channel in synaptic modification is compared in DG and CA1. 50 Hz train stimulus applied either perforant path-DG granule cell or Schaffer collateral-CA1 pyramidal cell pathways. I observed synaptic response by using an antibody to Kv4.1/Kv4.2 and found that Kv4.2 channel has the correlation with synaptic plasticity. My data demonstrates that inhibition of Kv4.2 induce enhancement with synaptic plasticity, whereas an anti-Kv4.1 antibody does not affect. This form of plasticity is different from the general long-term plasticity which was studied before.

The mechanisms underlying the effect on synaptic plasticity were investigated. It was observed that NMDA receptor blocker, APV, partially blocked potentiation in DG. However, a complete blockade of the potentiation occurred when nimodipine (L-type voltage-gated Ca^{2+} channel antagonist) was applied. In addition, PKC plays a crucial role in intracellular signaling cascades and its mechanisms thought to be involved in synaptic plasticity.

My results support the evidence of distinct density and distribution about Kv4.1 / Kv4.2 in DG and CA1 of the hippocampus. Furthermore, in this study, I clearly show that that synaptic plasticity that associated with Kv4.2 which is distinct from general synaptic plasticity and its mechanism.

Keywords : A-type K^+ current, Kv4.1, Kv4.2, synaptic plasticity, Long-term potentiation (LTP), DG granule cells, CA1 pyramidal cells

Student number : 2015-22026

CONTENTS

LIST OF FIGURES

Figures

Table

LIST OF ABBREVIATIONS

ACSF Artificial cerebrospinal fluid

AP Action potential

BAPTA 1,2-bis (o-aminophenoxy) ethane-N,N,N′,N′-tetraacetic acid

Ctrl Control

DG Dentate gyrus

DMSO Dimethyl sulfoxide

HEK Human embryonic kidney

K^+ Potassium ion

Kv Voltage-gated potassium

LTD Long-term depression

LTP Long-term potentiation

N.S Not significant

P Postnatal days

PKC Protein kinase C

SD Sprague-Dawley

TEA Triethanolamine

INTRODUCTION

Potassium (K^+) channels selectively transport K^+ across cell membranes and play a crucial role in physiological processes such as cell excitability, neurotransmitter release and signal transduction (O Pongs, 2008) K^+ currents are composed of multiple components with different kinetic properties. In particular, a transient outward K^+ current with a rapid activation and decay kinetics, which is called A-type voltage-gated potassium current, is well known in neurons to regulate neuronal excitability and firing frequency (B Liss et al., 2001; CC Lien and P Jonas, 2003; ZM Khaliq and BP Bean, 2008; J Johnston et al., 2010). The three types of voltage-gated potassium channel subunits, Kv4.2 and Kv4.3 which is encoded by the KCND / Kv4 channel family and Kv1.4, are known to mediate A-type K^+ current in heart and neurons (TJ Baldwin et al., 1991; MD Pak et al., 1991; P Serodio et al., 1996; SG Birnbaum et al., 2004; SB Long et al., 2005). Kv4.2 is the most significant contributor to A-type K^+ currents in the hippocampal neuron (M Martina et al., 1998; P Serodio and B Rudy, 1998; J Kim et al., 2005). Furthermore, Kv4.2 was shown to be expressed mainly in the dendrites with an increasing density from proximal to distal axis in CA1 pyramidal neurons (DA Hoffman et al., 1997; K Kerti et al., 2012) and the surface density of Kv4.2 in the synaptic sites is regulated when synaptic plasticity is induced (MH Kole et al., 2007; SC Jung et al., 2008; J Kim and DA Hoffman, 2008), suggesting its role in the regulation of synaptic intergration.

Kv4.1, another subunit that belongs to Kv4 channel family, has similar electrophysiological and pharmacological properties to those of Kv4.2 and Kv4.3 when expressed in heterologous expression systems (MD Pak et al., 1991), but the contribution of Kv4.1 to A-type K^+ currents in native neurons is not well understood. A recent study shows that Kv4.1 subunits are expressed in the hippocampus with the high expression level in the dentate gyrus granule cells

(Kim et al., 2016). Interestingly, subcellular localization of Kv4,1 is distinctive from that of Kv4.2, in that Kv4.1 is highly expressed only in the granule cell layer of the dentate gyrus with little expression in the molecular layer or in CA1 region, while Kv4.2 is highly expressed both in molecular layer of the dentate gyrus and stratum radiatum of CA1 region with little expression in the soma area. I hypothesized that due to different localization of Kv4.1 and Kv4.2 subunit, Kv4.1 and Kv4.2 channels may play different roles in synaptic responses.

'Synaptic plasticity' is a term used to describe persistent changes in synaptic strength. And such changes in the synaptic efficacy, including long-term potentiation (LTP) and long-term depression (LTD) which are considered as a physiological basis for one aspect of memory and learning, involve changes in AMPA receptor density in the synaptic sites (TV Bliss and GL Collingridge, 1993; MF Bear and RC Malenka, 1994; M Zhuo and RD Hawkins, 1995; RC Malenka and RA Nicoll, 1999; J Ster et al., 2009; GL Collingridge et al., 2010). The LTP is typically induced by high-frequency stimulation or by theta burst stimulation of presynaptic fibers, and this form of LTP requires Ca^{2+} influx via NMDA receptors into postsynaptic cells in the hippocampal CA1 region and dentate gyrus (DG). In addition to synaptic stimulation, LTP can be induced by the K^+ channel blocker tetraethylammonium (TEA) also induced synaptic potentiation (L Aniksztejn and Y Ben-Ari, 1991). TEA-induced LTP reported in the hippocampal CA1 region (YY Huang and RC Malenka, 1993; E Hanse and B Gustafsson, 1994; H Onuma et al., 1998) and DG (AN Coogan et al., 1999) is NMDA receptor-independent, but requires Ca^{2+} influx via L-type voltage-gated Ca^{2+} channel. These results suggest that increased Ca^{2+} signals induced by K^+ channel inhibition can regulate AMPA receptor density in synaptic sites. Considering that TEA is a non-specific K^+ channel blocker with a higher sensitivity for delayed rectifier K^+ currents, contribution of A-type K^+ currents to synaptic plasticity remains to be determined.

I investigated roles of Kv4.1 and Kv4.2 channels in excitatory postsynaptic responses of dentate granule cells and CA1 pyramidal cells in the hippocampus. I performed somatic patch-clamp recordings from DG/CA1 in acute hippocampal slices, and perfused anti-Kv4.1 antibody or anti-Kv4.1 antibody to selectively block Kv4.1 channels or Kv4.2 channels, respectively, to the cells through patch pipettes. I applied 50 Hz stimulation of PP/SC pathway with subthreshold intensity and observed postsynaptic excitability. In this study, I demonstrated that inhibition of Kv4.2 which gives rise to an enhancement of synaptic excitability is associated with synaptic plasticity. First, I tested whether the inhibition of Kv4.2 channels was dependent on NMDA receptors. In the results, the activation of L-type voltage-gated ca^{2+} channels but not NMDA receptors was required for the enhancement. In addition, the action of PKC was proposed as one of the underlying mechanisms of channel modulation by Kv4.2 antibody in this synaptic region.

These results strongly support a novel finding that modulation of A-type K^+ channels results in synaptic strength. Additionally, this finding suggests a possibility that the enhancement of synaptic plasticity through the inhibition of K^+ channels in hippocampal neurons, contributing to memory mechanisms as well as pathogenic conditions.

MATERIALS AND METHODS

HEK 293 cells culture

Monolayers of confluent HEK293 cells were cultured in Dulbecco's Modified Eagle's Medium (DMEM) with 3.7 g/L $NaHCO_3$ with addition of 2 mmol/L L-glutamine, 100 U/mL penicillin, and 100 mg/mL streptomycin and 10% fetal bovine serum in an atmosphere of 5% CO_2 95% air at 37C. Cells passages from 10 to 50 were used for experiments 4 to 10 days after trypsinization (0.05% trypsin and 0.02% EDTA in Mg^{2+}, Ca^{2+}free phosphate buffer).

DNA transfection

For transfection, Kv4.1 / Kv4.2 DNA into HEK 293 cells was performed using Lipofectamine 2000 (Invitrogen) according to the instruction of the manufacturer. All experiments were recording in HEK 293 cells within 50 passages. HEK 293 cells after transfected were maintained in a incubator at 37℃ with 1% O_2 for 6 or 12 h. Cells transfected 1 or 2 days before the experiment were used for electrophysiological recordings.

Animals and ethical approval

All animal studies and experimental protocols were approved by the Institutional Animal Care and Use Committee (IACUC) at Seoul National University. The animals were maintained in standard environmental conditions (25 ± 2 ℃; 12/12 h dark/light cycle) and were housed under veterinary supervision at the Institute for Experimental Animals, Seoul National University College of Medicine.

Hippocampal slice preparation and electrophysiological recordings

Transverse hippocampal slices (300 mm) were prepared from Sprague–Dawley rats (P16 – P19 of either sex. Rats were anesthetized with diethyl ether and killed by decapitation, and brains were quickly removed and placed in ice-cold artificial cerebrospinal fluid (aCSF) containing (in mM): 116 NaCl, 3.2 KCl, 1.25 NaH_2PO_4, 26 $NaHCO_3$, 0.5 $CaCl_2$, 7 $MgCl_2$, 10 Glucose, 2 Na-pyruvate, 3 vitamin C bubbled with mixture of 95% O_2–CO_2. Slices were recovered for 1 h at 32 C before use. Whole-cell voltage- or current-clamp recordings from hippocampal CA1 pyramidal cells and DG granule cells were performed at 32 ± 1℃ and the rate of aCSF perfusion was maintained at 1–1.5 ml /min. The recordings were made in somata with EPC-8 amplifier (HEKA Electronik) at a sampling rate of 10 kHz. Patch pipettes (3– 4 MΩ for somatic recording) were filled with internal solutions containing the following (in mM): 130 potassium gluconate, 7 KCl, 2 NaCl, 1 $MgCl_2$, 0.1 EGTA, 2 ATP-Mg, 0.3 Na-GTP, 10 HEPES adjusted to pH7.3 with KOH. In whole-cell recordings, we used a aCSF containing the following (in mM): 124 NaCl, 26 $NaHCO_3$, 3.2 KCl, 1.25 NaH_2PO_4, 2.5 $CaCl_2$, 1.3 $MgCl_2$, 10 glucose bubbled with mixture of 95% O_2, 5% CO_2 to a final pH of 7.4. Monopolar electrodes (tip size: 2-3 μm) filled with aCSF were connected to the stimulator (Master-8, AMPI, Jerusalem, Israel). EPSP and EPSC were recorded in DG or CA1 neurons. After patch break-in, control EPSP/EPSC (50 Hz, 2 min) are measured. EPSPs/EPSCs are recorded again 15minutes later for comparison. A stimulation electrode was placed at apporximately 100μm or 300μm away from the granule cell layer in DG. On the other hand, in CA1, a stimulation electrode was placed at apporximately 150μm or 400μm away from the recording site to stimulate the Schaffer Collateral fibers.

Drug treatment

All pharmacological compounds were made up in stock solutions at concentration 100–1000 times higher than those required and diluted in the ACSF solutions as appropriate immediately before use. Bicuculline (20 μM) was purchased from from abcam Biochemicals (Cambridge, UK) and APV (50 μM) was from Tocris Bioscience. GF-109203X (5 μM) and bisindolylmaleimide V (5 μM) (inactive analogue of GF-109203X) were purchased from Santa Cruz Biotechnology. All other drugs were purchased from Sigma-Aldrich. Stock solutions of drugs were made by dissolving in deionized water or DMSO according to manufacturer's specifications and were stored at -20℃. On the day of the experiment one aliquot was thawed and used. The concentration of DMSO in solutions was maintained at 0.1%.

Statistical analysis

Data were analyzed using IgorPro (version 6.1, WaveMetrics), OriginPro (version 8.0, Microcal) software, and are presented as mean ± SEM, where n represents the number of cells studied. The statistical significance of differences between two groups was evaluated using a Student's t-test with confidence levels of $p < 0.01$ (**), $p < 0.05$ (*) and $p > 0.05$ (not significant, n.s).

RESULTS

Identifying the efficacy of antibody on K^+ current in HEK 293 cells.

Before conducting a full-scale experiment in the hippocampal slice, an antibody test experiment was performed using a specific antibody against Kv4.1 to confirm the efficacy of antibody in the HEK 293 cells (Fig. 1A). I investigated this test in Kv4.1/4.2 transfected cells by analyzing the effect on K^+ current. In this part of the study, I used cell passages from 10 to 50 with 10% fetal bovine serum. HEK 293 cell cultures were maintained in DMEM and cells were transfected by seeding 1 × 105 cells in 12 well 1 or 2 days prior to the experiment. After the Kv4.1 / Kv4.2 DNA transfection, Kv4.1 or Kv4.2 channels were over-expressed in Hek293 cells, respectively. By whole-cell patch clamp recording K^+ currents were recorded in voltage-clamp mode by applying a 40mV depolarizing pulse (500ms) from a holding potential at -80 mV. Kv4.1/4.2 current recorded in HEK293 cells displayed rapid activation and inactivation kinetics, typically observed in A-type K^+ currents (SG Birnbaum et al., 2004).

To directly test the contribution of antibody to the K^+ current, I added a specific antibody to Kv4.1 / 4.2 (6 μg/ml) (H Murakoshi and JS Trimmer, 1999) to the pipette solutions respectively and recorded the changes in peak amplitude of K^+ currents during intracellular dialysis with the anti-Kv4.1 antibody. Current amplitudes were plotted against the time duration after patch break-in. These data show that Kv4.1 current decreased gradually by an anit-Kv4.1 antibody, whereas Kv4.2 current was sustained with a steady state. To directly compare the difference in peak current between Kv4.1 transfected cell and Kv4.2 transfected cell with an anti-Kv4.1 antibody, normalized peak current were superimposed (Fig. 1B, Kv4.1 current; n = 9, Kv4.2 current; n = 8).

I further executed the same experiment with anti-Kv4.2 antibody. I used anti-Kv4.2 antibody-containing pipette solutions in voltage-clamp recordings. I monitored the changes in K^+ current of between Kv4.1 transfected cell and Kv4.2 transfected cell while antibodies were diffused into the cells after patch break-in. A marked change was observed with gradual decrease in peak amplitude in Kv4.2 transfected cell with anti-Kv4.2 antibody (Fig. 1D, Kv4.1 current; n = 6, Kv4.2 current; n = 5). During the initial three minutes, the cell-to-cell variation appears considerably. If I normalize current without consideration of this difference with cells, there is a problem with the effect caused by antibody will under-estimated. For the most reasonable analysis, I estimated baseline by extrapolation from constant slope and normalized. Next, I conducted an experiment using the antibody in the hippocampal slice.

Inhibition of Kv4.1 enhances neuronal excitability in proximal site of DG, but not in distal site.

Kv4 family channels mediate A-type K^+ currents, which are crucial for regulating neuronal excitability. To identify the roles of Kv4.1 in synaptic response between the two cell types, I performed a series of antibody experiments in hippocampal neurons in DG and CA1. EPSP were recorded using a whole cell current clamp technique with a recording electrode located at the soma containing a specific antibody to Kv4.1 (1.5 μg/ml) (H Murakoshi and JS Trimmer, 1999). To monitor the effect of Kv4.1 antibody on EPSPs, I monitored changes in EPSPs during antibody diffusion. Figure 2 shows a experimental protocol for testing antibody effects. EPSPs were evoked by 5 train pulses with 50 Hz (Fig. 2A) with stimulating electrodes positioned about 150 μm or 400 μm away from the soma to stimulate proximal or distal input, repectively (Fig. 2B). When stable recording conditions were obtained, which was usually about 3 min after making whole cell, I applied stimulations in a 5 s interval to continuously monitor changes

in EPSPs. A representative plot for changes in the amplitude of EPSPs is shown in Figure 2A (Fig. 2A, right, open purple circles). I regarded the average of 1 minute recording as control. When the changes in EPSPs due to antibody diffusion reached the steady state, approximately 15 minutes after patch break-in, the average of 1 minute was obtained again. This value was compared with the control value. And the difference was regarded as the effect of the antibody. I confirmed that under my experimental conditions, EPSP amplitude remained unchanged when control internal solutions without antibody were used (Fig. 2A, right, open black squares).

Image of hippocampal slice with stimulating electrode and recording electrode are shown in Figure 2B. As shown in Figure 2Ba and 2Bc, a stimulating electrode is positioned in the molecular layer or stratum radiatum about 400 μm away from the soma of DG and CA1. Proximal site stimulation in the DG/CA1 which was done about 150 μm away from the soma also executed (Fig. 2Bb and 2Bd).

In the presence of Bicuculline (20 μM), I applied 50 Hz stimulus train to Perforant Pathway (PP) with subthreshold intensity that could evoke EPSP. First, this stimulation was applied in the distal dendrites of DG granule cells, and repeated every 5 seconds with constant intensity. I recorded control responses within 3 minutes after whole-cell and labeled anti-Kv4.1 which were recorded 15 minutes after whole-cell. In Figure 3Ba, EPSP representative raw traces are shown in control (black) and anti-Kv4.1(red). I first tested whether excitatory postsynaptic potentials (EPSPs) evoked by distal PP stimulations are altered after sufficiently diffused antibody. As shown in bar graph, the average of amplitudes of the 1st EPSP was slightly increased with the ratio of 1.31 (Fig. 3Bb, 1.31 ± 0.20, $p > 0.05$, $n = 6$). But there was no significant difference between control and antibody in the 1st EPSP amplitude with distal dendrite stimulation. Next, I applied stimulation to perforant pathway in the proximal apical dendrites of DG granule cells (Fig. 3Ca). In contrast with distal PP stimulation in DG, the

amplitudes of the 1st EPSP were significantly increased with the ratio of 1.56 (Fig. 3Bb; 1.56 ± 0.20, $p < 0.05$, $n = 8$).

I also executed the same experiment in hippocampal CA1 pyramidal cells (Fig. 4A). Schaffer collateral pathway stimulation applied in the distal apical dendrites of CA1 pyramidal cells, then evoked EPSP (Fig. 4Ba). Likewise, 50 Hz stimulation was repeated every 5 seconds with constant intensity. As can be seen, there was no significant difference in control and anti-Kv4.1 (Fig. 4Bb; 1.13 ± 0.11, $p > 0.05$, $n = 7$). Likewise, there was no marked difference in the 1st EPSP amplitude with proximal dendrite stimulation (Fig. 4Cb; 1.13 ± 0.09, $p > 0.05$, $n = 9$). In contrast with DG, there was no significant difference in control and anti-Kv4.1 on the 1st EPSP amplitude at the stimulus of two positions in CA1.

Whether or not Kv4.1 antibody will have an impact on EPSC, I also analyzed the 1st EPSC in the same manner. To clearly view differences, both bar graph and cumulative EPSC were listed simultaneously. The 1st EPSC amplitude and cumulative EPSC at the stimulus of two positions sustained without significant changes in the amplitude (Fig.5Ba; 1.01 ± 0.77, $p > 0.05$, $n = 6$, Fig. 5Bb; 0.98 ± 0.07, $p > 0.05$, $n = 4$). I performed the same series of experiments in CA1 pyramidal cells and recorded the amplitude of EPSC. Likewise with DG, EPSC which were recorded in the distal dendrite are shown without significant changes in the amplitude (Fig. 5Da; 1.02 ± 0.09, $p > 0.05$, $n = 6$). Then, I recorded EPSC evoked by 50 Hz stimulation in the proximal dendrite in the same way. As expected, PP stimulation with proximal dendrite never changed in EPSC amplitude (Fig. 5Db; 0.92 ± 0.05, $p > 0.05$, $n = 5$).

Judging from the previous results in Figure 5, I found that the anti-Kv4.1 antibody did not significantly affect any of these EPSC data. To sum up, excitatory postsynaptic potential (EPSP) of DG granule cells in the presence of the anti-Kv4.1 antibody was significantly higher than that obtained from data in the absence of the anti-Kv4.1 antibody. These results suggest that

inhibition of Kv4.1 does not affect in synaptic response in current, but affect very little in neuronal excitability in DG.

In summary, the effectiveness of Kv4.1 in synaptic modification was compared for dentate gyrus and CA1 by recording from both sites of hippocampal slice. I confirmed that the resting membrane potentials remained unchanged after antibody perfusion (data not shown). The amplitude of EPSP in proximal recording in DG, measured 15-20min following antibody perfusion, was increased. The amplitude of this increasement was 1.56 of baseline. In contrast to the effects of Kv4.1 in DG, slight but non-significant enhancement was induced in CA1 following antibody perfusion. A marked differential effect of Kv4.1 was observed on the EPSP profile during Kv4.1 antibody perfusion. Comparison of averaged EPSP evoked by 50 Hz train stimulus in the absence and presence of antibody showed that the 1st EPSP in DG largely affected by anti-Kv4.1 antibody, but EPSP in CA1 was not significantly affected.

This result is consistent with the previous study that showing a high density of Kv4.1 DG. However, consistent with the EPSC result in DG, amplitude of EPSC was no effect in CA1 measured 15 minutes after antibody perfusion. The 1st EPSC amplitude and cumulative EPSC data showed that there was no significant effect in dendritic Ca^{2+}.

EPSCs are potentiated by inhibition of Kv4.2 at distal dendrites, but not at proximal dendrites.

In the second place, to understand of the Kv4.2 subunit of A-type K channel, I executed the antibody test of Kv4.2. This time, I added a specific antibody to Kv4.2 (1.5 μg/ml) (Murakoshi H and JS Trimmer, 1999) to the pipette solutions at the soma, and a stimulating electrode was placed on the molecular layer of DG (Fig. 6A). In case that recorded with

stimulation in distal apical dendrite in DG, the 1st EPSP showed approximately two-fold increase in comparison with the control (Fig. 6Bb; 1.82 ± 0.26, $p < 0.05$, $n = 6$). On the other hand, PP stimulation in proximal apical dendrite showed that the 1st EPSP was slightly increased, but were negligible (Fig. 6Cb; 1.39 ± 0.22, $p > 0.05$, $n = 6$).

To investigate whether this impact is reproducible in the different region, I tested the same experiment in CA1 (Fig. 7A). As the same result with DG, inhibition of Kv4.2 of distal dendrite in CA1 significantly affect the 1st EPSP. The response showed the steep increase in EPSC amplitude. The degree of EPSP increment is shown in Figure 7Bb (1.41 ± 0.12, $p < 0.01$, $n = 8$). I subsequently examined EPSP with proximal dendrite stimulation in CA1 (Fig. 7Ca). But the 1st EPSP amplitude remains without significant change (Fig. 7Cb; 1.22 ± 0.22, $p > 0.05$, $n = 6$).

Like a test in Kv4.1, I also analyzed the 1st EPSC and cumulative EPSC in the same manner whether to make changes to response in EPSC. I found the results that unseen before experiment. Unlike the result in anti-Kv4.1 shown in Figure5, inhibition Kv4.2 channel by using anti-Kv4.2 antibody induced synaptic potentiation. The amplitude of EPSC, measured 15 to 20 minutes after antibody perfusion, was 1.56 ± 0.14 of the baseline (Fig. 8Bb; $p < 0.01$, $n = 10$). As expected, Recording with proximal stimulus had no significantly different response on the EPSC in DG (Fig. 8Cb; 1.10 ± 0.06, $p > 0.05$, $n = 9$). This enhancement in EPSC amplitude showed the same in CA1. A marked increasement of EPSC was observed in recording with the distal stimulus (Fig. 8Da; 1.64 ± 0.13, $p < 0.01$, $n = 10$) whereas no impact on recording with the proximal stimulus (Fig. 8Db; 1.06 ± 0.05, $p > 0.05$, $n = 8$).

To sum up, these results informed that effect by anti-Kv4.2 antibody involves not only the EPSP but also the EPSC. These results indicate that Kv4.2 should be contributable to dendritic Ca^{2+} signaling. Also, this result is consistent with the previous study showing that a gradual

increase of Kv4.2 density along the proximo-distal axis of dendrites. I then investigated whether Kv4.2-dependent synaptic enhancement involves a specific mechanism.

This potentiaion does not depend on synaptic stimulation.

I was wondering if this potentiation was related to synaptic stimulation, because the previous experiment was executed with repetitive stimulation every 5 seconds. So I measured the control for the first 1 minute and recorded the EPSC again after about 15 minutes without repetitive stimulation, to see if the result differs from the previous experiment. The EPSC amplitude with an antibody to Kv4.2 which was obtained from previous experiment was plotted with time in Figure 9A, and the first and last recorded EPSC amplitude without stimulation was also superimposed. In Figure 9B, the average of EPSC amplitude was shown in blue (no stim) and black (stim), respectively. As shown in bar graph, there was no significant difference in the value depending on the stimulus. The normalized amplitude was almost the same with or without repetitive stimulation (Fig. 9B, no stim; 1.48 ± 0.06, n=3, stim; 1.56 ± 0.14, n=10, $p > 0.05$). Consequently, I confirmed that this potentiation does not depend on synaptic activity.

Synaptic potentiation at distal dendrites in DG is mediated by L-type voltage-gated Ca^{2+} channel.

To understand mechanisms of this potentiation in the distal dendrite, I measured only EPSC amplitudes against the time after patch break-in (Fig. 10). The data from all of the experiments in which were applied any pharmacological manipulations are shown in Figure 9 and Figure 10.

Synaptic potentiation of the hippocampus is critically dependent on arising in the postsynaptic calcium concentration (Nicoll and Malenka, 1999). And, this initial rise in calcium levels triggers the signaling cascade that ultimately leads to increased synaptic efficacy. In agreement with these earlier evidences, I first examined the ability of the synaptic potentiation by using APV (50μM) to block NMDA receptor to determine the contribution of NMDA receptor to the potentiation. As can be seen in Figure 9Ba, Recordings showed that APV did not alter the amplitude of the baseline EPSC. APV partially blocked the induction of Kv4.2-dependent potentiation but not significant (Fig. 10C, 1.50 ± 0.20, $p > 0.05$, $n = 4$). The addition of APV resulted in a sustained potentiation of EPSC amplitudes, suggesting that NMDA receptor may be not involved mainly of this form of potentiation. In other words, the potentiation triggered by inhibition of Kv4.2 was not totally abolished.

Another candidate is the L-type voltage-gated Ca^{2+} channel. So, I examined the effect of nimodipine (10μM), an L-type voltage-gated Ca^{2+} channel antagonist, on EPSC amplitude. The amplitude of EPSC in DG, measured at 15 miutes after antibody perfusion, was 1.20 of baseline (Fig. 10C, 1.20 ± 0.10, $p < 0.05$, $n = 8$). In pretreatment with nimodipine, the increase in the amplitude of EPSC was suppressed, whereas the recorded after the application of APV did not affect significantly. The time course of EPSC under blockade of L-type voltage-gated Ca^{2+} channel are shown in Figure 10Bb. As shown in this result, the L-type voltage-gated Ca^{2+} channels are involved in this form of potentiation. If Ca^{2+} influx into postsynaptic cells is required for Kv4.2 induced synaptic potentiation, further studies are needed to reveal the involvement of postsynaptic Ca^{2+} influx using the injection of a Ca^{2+} chelator such as BAPTA. To confirm this mechanism, 10 mM BAPTA was added in the internal recording solution and recorded EPSC again only in the presence of bicuculline. As expected, preventing the rise in cytosolic Ca^{2+} levels by including the calcium chelator BAPTA in the pipette also resulted in

the complete block of potentiation (Fig. 10C, 1.01 ± 0.08, $p < 0.05$, $n = 6$). The control and potentiated mean EPSC of these observations are superimposed in Figure 10Bc. Thus, it is concluded that LTP in distal dendrite is mediated by L-type Ca^{2+} signaling.

PKC is involved in the novel form of synaptic plasticity.

It has been reported that L-type Ca^{2+}channels have several downstream events interacting with PKC (GM Ramakers et al., 2000). These previous studies support the hypothesis that PKC is involved in the pathway of L-type Ca^{2+} channel dependent synaptic potentiation. The role of PKC in the Kv4.2 LTP in DG was investigated.

To test this hypothesis, similar studies were carried out in slices pretreated with GF-109203X (inhibitor of PKC, also known as bisindolylmaleimide I, 5μM) or its inactive analogue, bisindolylmaleimide V (5μM). GF-109203X is a competitive inhibitor of ATP binding and is highly selective for PKC (D Toullec et al., 1991; A Baron et al., 1993). In GF-109203X pre-treated recording, the increase in EPSC amplitude was not observed (Fig. 11Ba), while bisindolylmaleimide V did not suppress synaptic potentiation (Fig. 11Bb). The bar graph of relative EPSC amplitude is in Figure10C (GF-109203X; 0.90 ± 0.06, $p < 0.01$, $n = 5$, BIM V; 1.48 ± 0.09, $p > 0.05$, $n = 3$). These findings suggested that PKC is strongly involved in synaptic transmission of hippocampal neurons by an L-type voltage-gated Ca^{2+} channel-dependent mechanism.

Eventually, my study supports the emerging consensus that rises in intracellular Ca^{2+} lead to increases in synaptic efficacy. The increase in EPSC amplitudes triggered by inhibition of Kv4.2 is mediated by Ca^{2+} signaling cascade that involves PKC pathway via the L-type Ca^{2+} channel. The ability to induce change throughout the modulation of K^+ channel is specific to

Kv4.2 and this novel finding provides a possibility to alterations in synaptic strength.

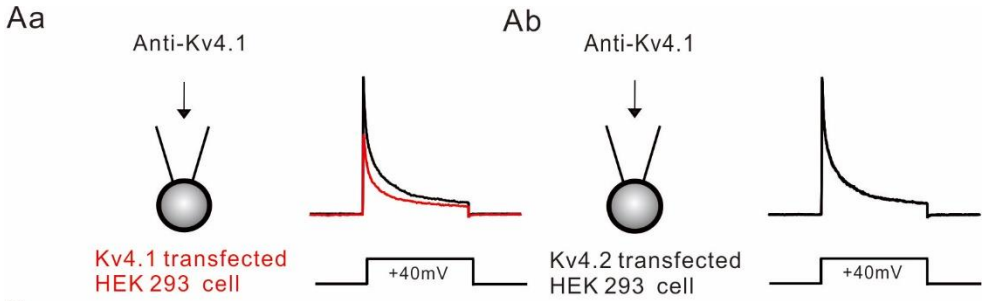
Aa
Anti-Kv4.1
Kv4.1 transfected
HEK 293 cell
+40mV
Ab
Anti-Kv4.1
Kv4.2 transfected
HEK 293 cell
+40mV

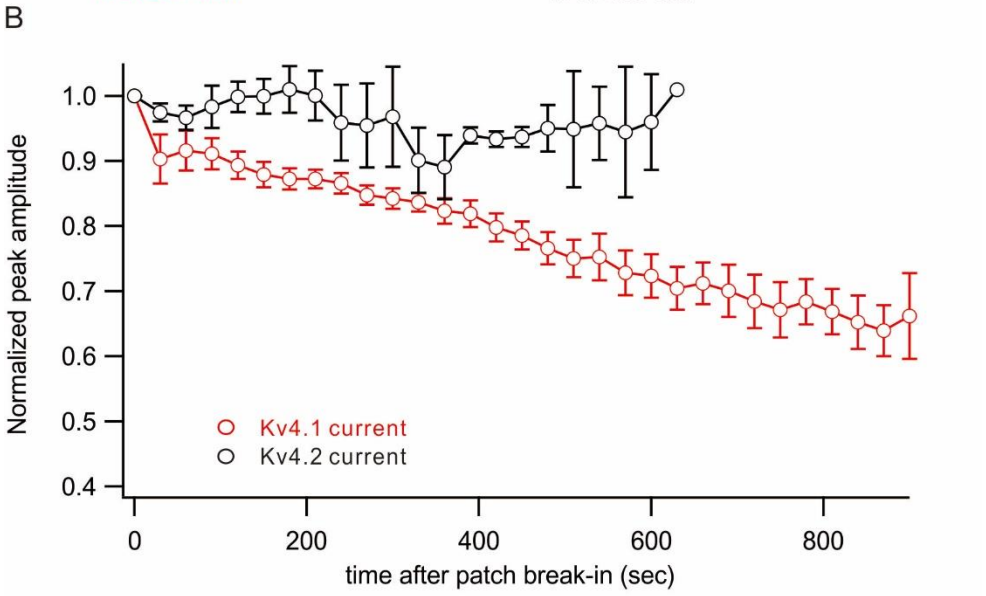
B
Normalized peak amplitude
1.0
0.9
0.8
0.7
0.6
0.5
0.4
Kv4.1 current
Kv4.2 current
0
200
400
600
800
time after patch break-in (sec)

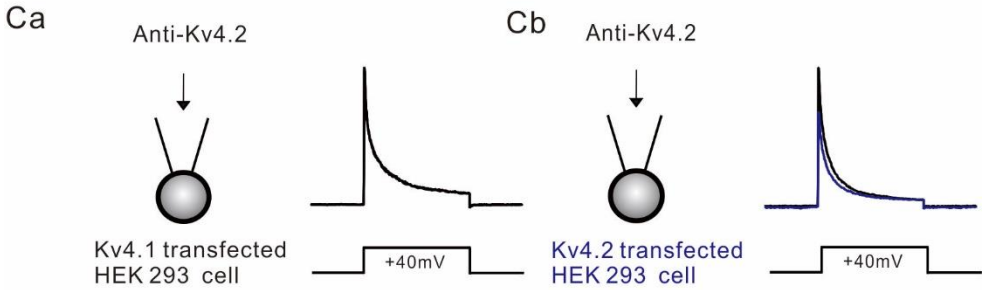
Ca
Anti-Kv4.2
Kv4.1 transfected
HEK 293 cell
+40mV
Cb
Anti-Kv4.2
Kv4.2 transfected
HEK 293 cell
+40mV

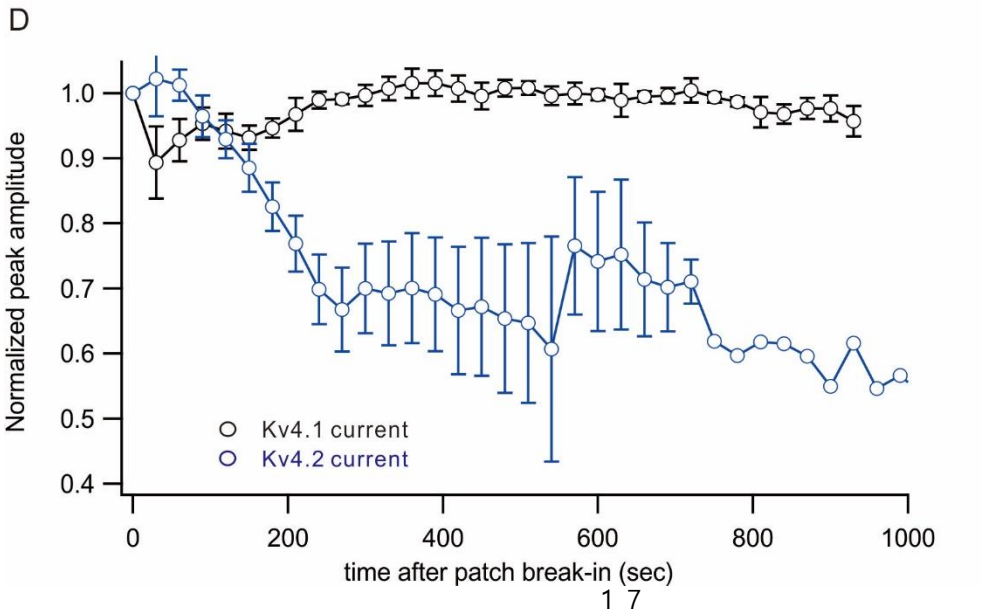
D
Normalized peak amplitude
1.0
0.9
0.8
0.7
0.6
0.5
0.4
Kv4.1 current
Kv4.2 current
0
200
400
600
800
1000
time after patch break-in (sec)

Figure 1. Identifying the efficacy of antibody on K^+ current in HEK 293 cells.

(Aa) Representative trace of the impact of the anti-Kv4.1 antibody on K^+ current evoked by depolarizing pulse to +30 mV in Kv4.1 transfected HEK 293 cell.

(Ab) Representative trace of the impact of the anti-Kv4.1 antibody on K^+ current evoked by depolarizing pulse to +30 mV in Kv4.2 transfected HEK 293 cell.

(B) Normalized peak current in Kv4.1 transfected cell (n = 9) and Kv4.2 transfected cell (n = 8) with anti-Kv4.1 antibody were superimposed.

(Ca) Representative trace of the impact of the anti-Kv4.2 antibody on K^+ current evoked by depolarizing pulse to +30 mV in Kv4.1 transfected HEK 293 cell.

(Cb) Representative trace of the impact of the anti-Kv4.2 antibody on K^+ current evoked by depolarizing pulse to +30 mV in Kv4.2 transfected HEK 293 cell.

(D) Normalized peak current in Kv4.1 transfected cell (n = 6) and Kv4.2 transfected cell (n = 5) with anti-Kv4.2 antibody were superimposed.

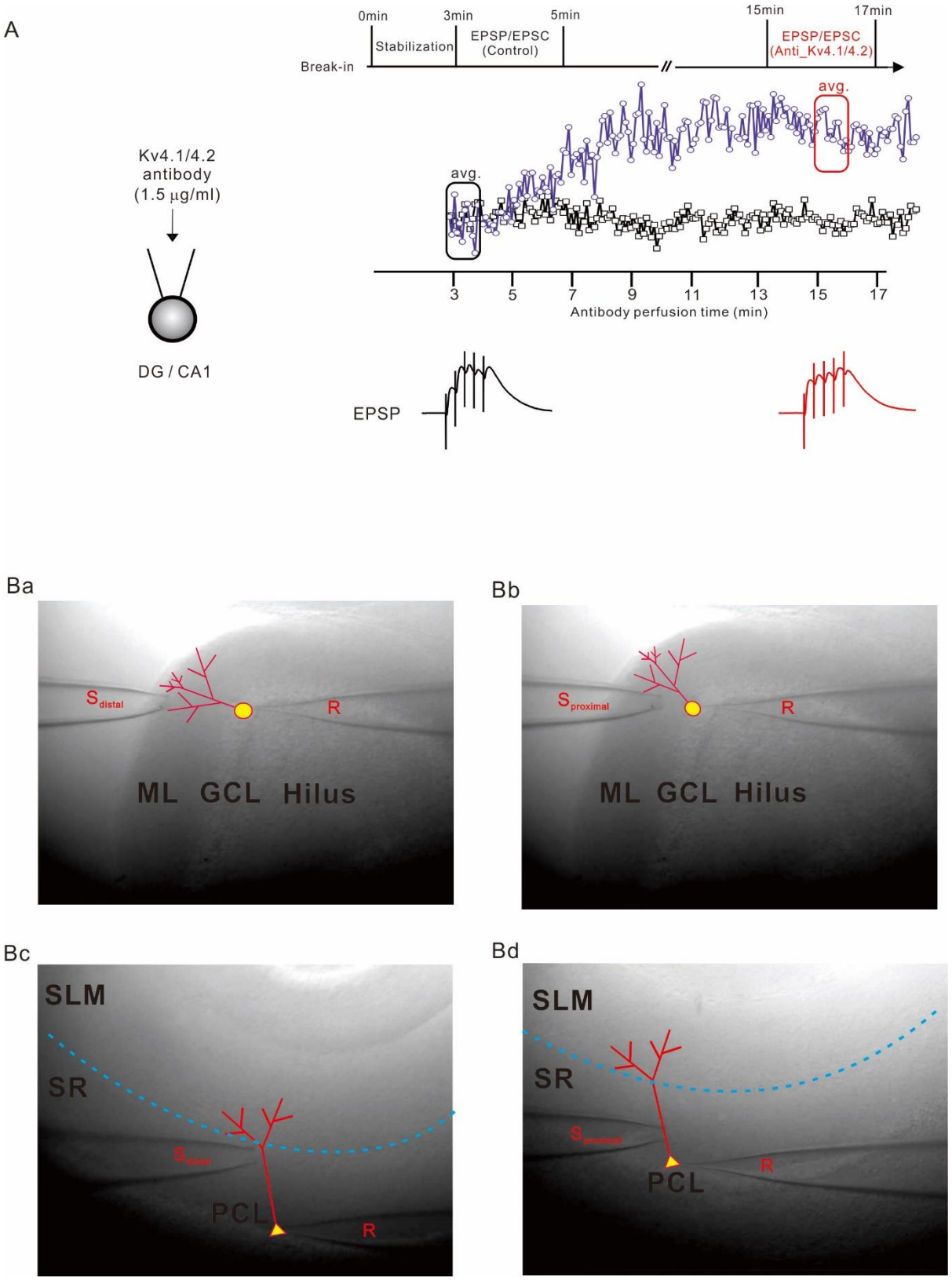
A
0min
3min
5min
15min
17min
Stabilization
EPSP/EPSC
(Control)
EPSP/EPSC
(Anti_Kv4.1/4.2)
Break-in
avg.
avg.
Kv4.1/4.2
antibody
(1.5 μg/ml)
3
5
7
9
11
13
15
17
Antibody perfusion time (min)
DG / CA1
EPSP
Ba
Bb
S distal
R
ML GCL Hilus
S proximal
R
ML GCL Hilus
Bc
Bd
SLM
SR
S distal
PCL
R
SLM
SR
S proximal
PCL
R

Figure 2. Experimental methods and image of the hippocampal slice with a stimulating electrode and recording electrode.

(A) Diagram illustrating the timeline for the experiment.

(Ba) Image of the hippocampal slice with stimulating electrode and recording electrode located in the hippocampal DG region. A stimulating electrode is positioned in the molecular layer about 400 μm away from the soma of the cell.

(Bb) Image of the hippocampal slice with stimulating electrode and recording electrode located in the hippocampal DG region. A stimulating electrode is positioned in the molecular layer about 150 μm away from the soma of the cell.

(Bc) Image of the hippocampal slice with stimulating electrode and recording electrode located in the hippocampal CA1 region. A stimulating electrode is positioned in the stratum radiatum about 400 μm away from the soma of the cell.

(Bd) Image of the hippocampal slice with stimulating electrode and recording electrode located in the hippocampal CA1 region. A stimulating electrode is positioned in the stratum radiatum about 150 μm away from the soma of the cell.

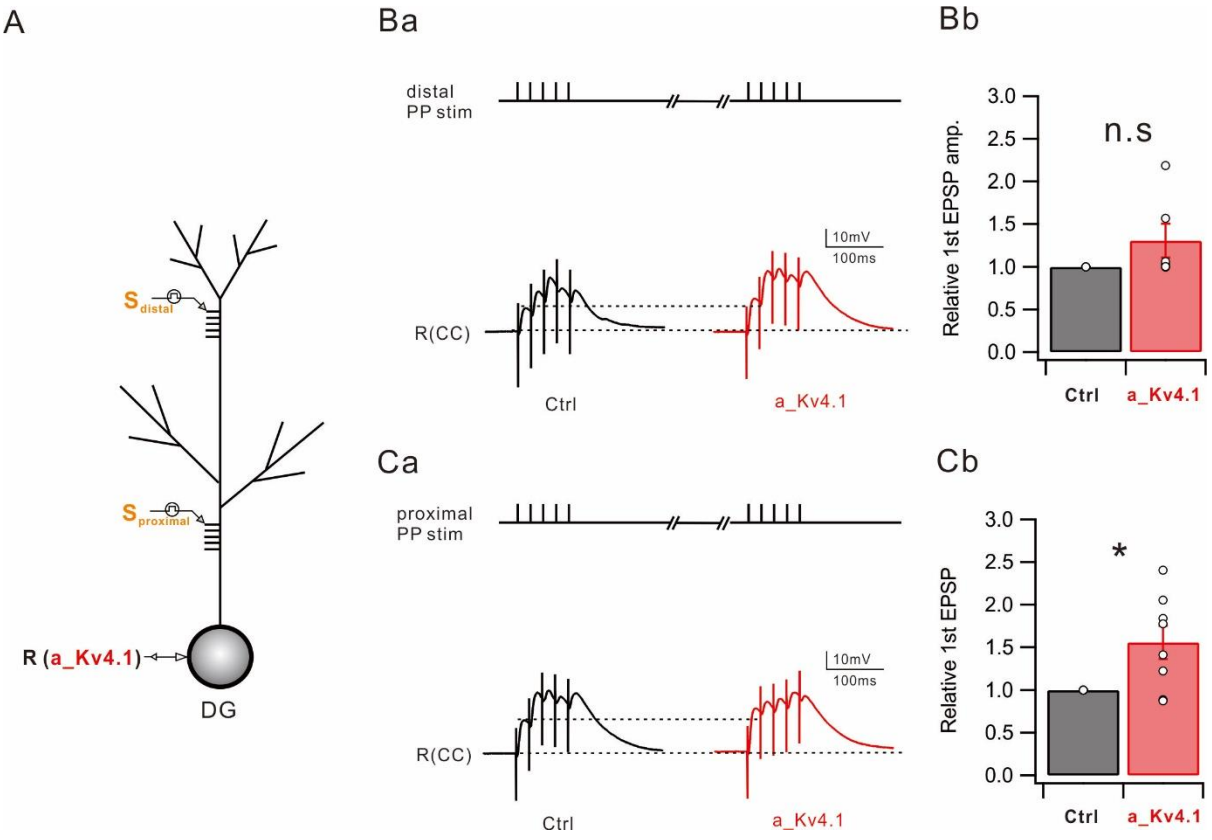

Figure 3. Kv4.1 contributes to the EPSP in proximal site of DG, but not in distal site.

(A) Experimental configurations showing whole-cell recording with stimulation at distal and proximal dendrite in DG.

(Ba) Representative traces of summated EPSP recorded from soma in response to 50 Hz stimulation at distal dendrites before (black) and after (red) anti-Kv4.1 antibody perfusion.

(Bb) Bar graphs summarize relative amplitude of the 1st EPSP (n = 6) in control (black) and after anti-Kv4.1 antibody perfusion (red).

(Ca) Representative traces of summated EPSP recorded from soma in response to 50 Hz stimulation at proximal dendrites before (black) and after (red) anti-Kv4.1 antibody perfusion.

(Cb) Bar graphs summarize relative amplitude of the 1st EPSP (n = 8) in control (black) and

after anti-Kv4.1 antibody perfusion (red).

n.s, $p > 0.05$, *, $p < 0.05$, **, $p < 0.01$. Circles represent data from individual experiments and bars indicate mean ± SEM.

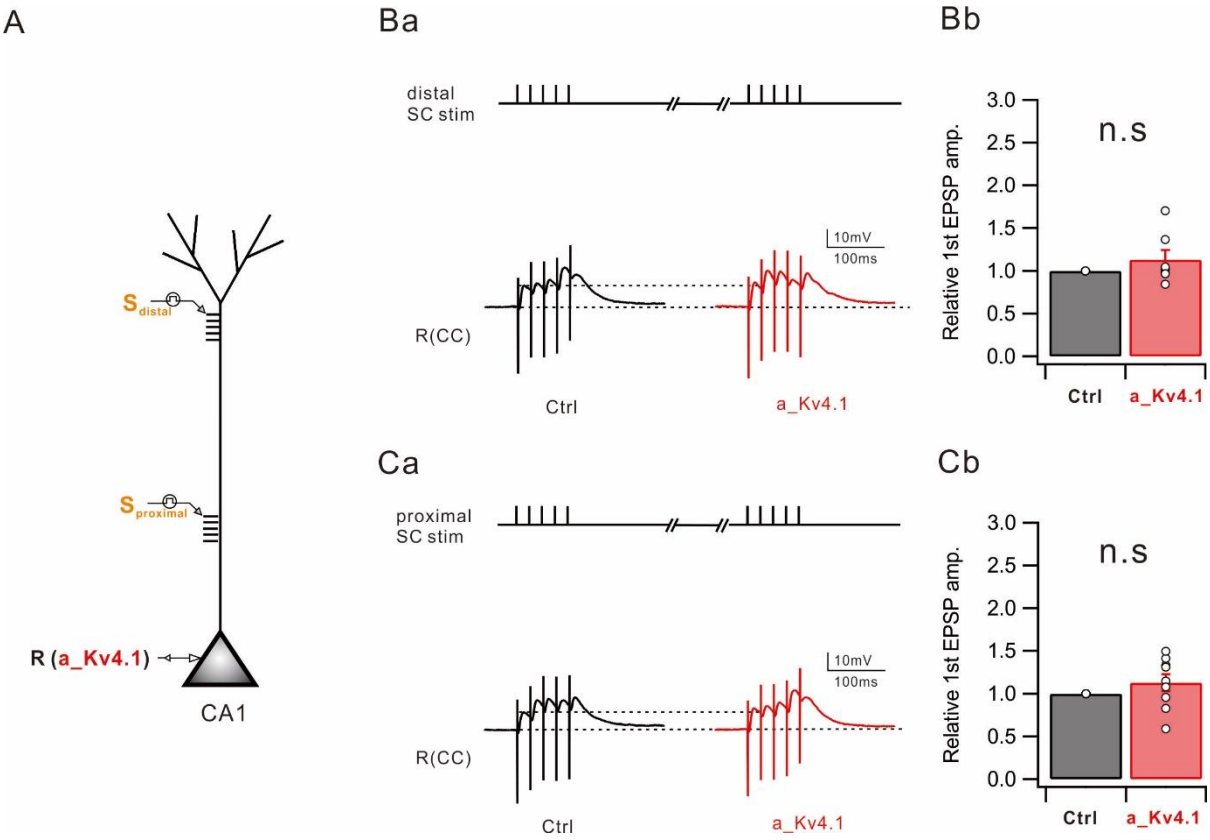

Figure 4. Non-significant effects on EPSP with anti-Kv4.1 antibody in CA1.

(A) Experimental configurations showing whole-cell recording with stimulation at distal and proximal dendrite in CA1.

(Ba) Representative traces of summated EPSP recorded from soma in response to 50 Hz stimulation at distal dendrites before (black) and after (red) anti-Kv4.1 antibody perfusion.

(Bb) Bar graphs summarize relative amplitude of the 1st EPSP (n = 7) in control (black) and after anti-Kv4.1 antibody perfusion (red).

(Ca) Representative traces of summated EPSP recorded from soma in response to 50 Hz stimulation at proximal dendrites before (black) and after (red) anti-Kv4.1 antibody perfusion.

(Cb) Bar graphs summarize relative amplitude of the 1st EPSP (n = 9) in control (black) and

after anti-Kv4.1 antibody perfusion (red).

n.s, $p > 0.05$, *, $p < 0.05$, **, $p < 0.01$. Circles represent data from individual experiments and bars indicate mean ± SEM.

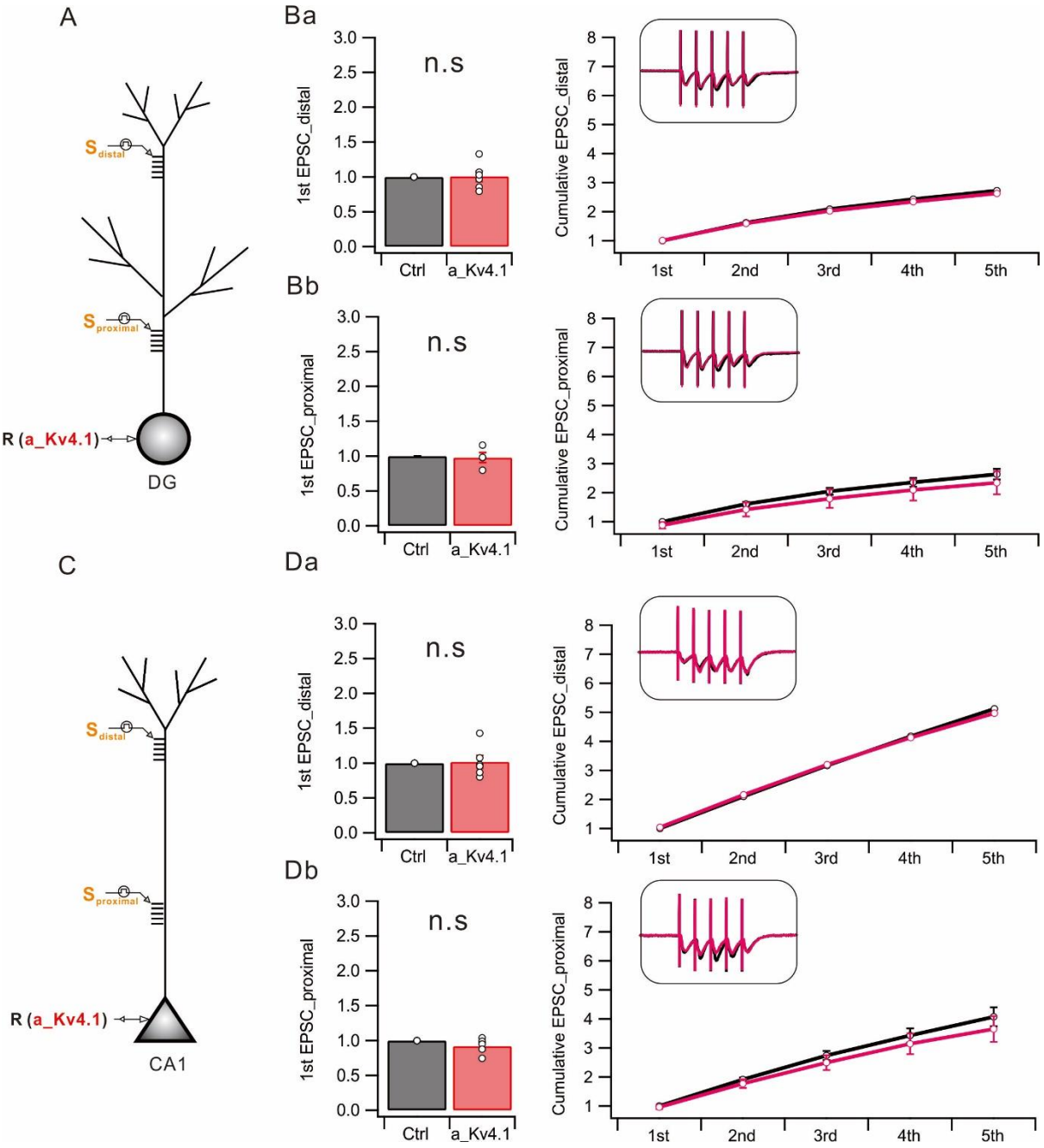

Figure 5. EPSC was not affected by anti-Kv4.1 antibody in DG and CA1.

(A) Experimental configurations showing whole-cell recording with stimulation at distal and proximal dendrite in DG.

(Ba) Left, summary data showing normalized the 1st EPSC amplitude by stimulation at distal

dendrites in control (black) and anti-Kv4.1 (red) (n = 6). Right, averaged cumulative EPSC in response to stimulation.

(Bb) Left, summary data showing normalized the 1st EPSC amplitude by stimulation at proximal dendrites in control (black) and anti-Kv4.1 (red) (n = 4). Right, averaged cumulative EPSC in response to stimulation.

(C) Experimental configurations showing whole-cell recording with stimulation at distal and proximal dendrite in CA1.

(Da) Left, summary data showing normalized the 1st EPSC amplitude by stimulation at distal dendrites in control (black) and anti-Kv4.1 (red) (n = 6). Right, averaged cumulative EPSC in response to stimulation.

(Db) Left, summary data showing normalized the 1st EPSC amplitude by stimulation at proximal dendrites in control (black) and anti-Kv4.1 (red) (n = 5). Right, averaged cumulative EPSC in response to stimulation. n.s, $p > 0.05$, *, $p < 0.05$, **, $p < 0.01$. Circles represent data from individual experiments and bars indicate mean ± SEM.

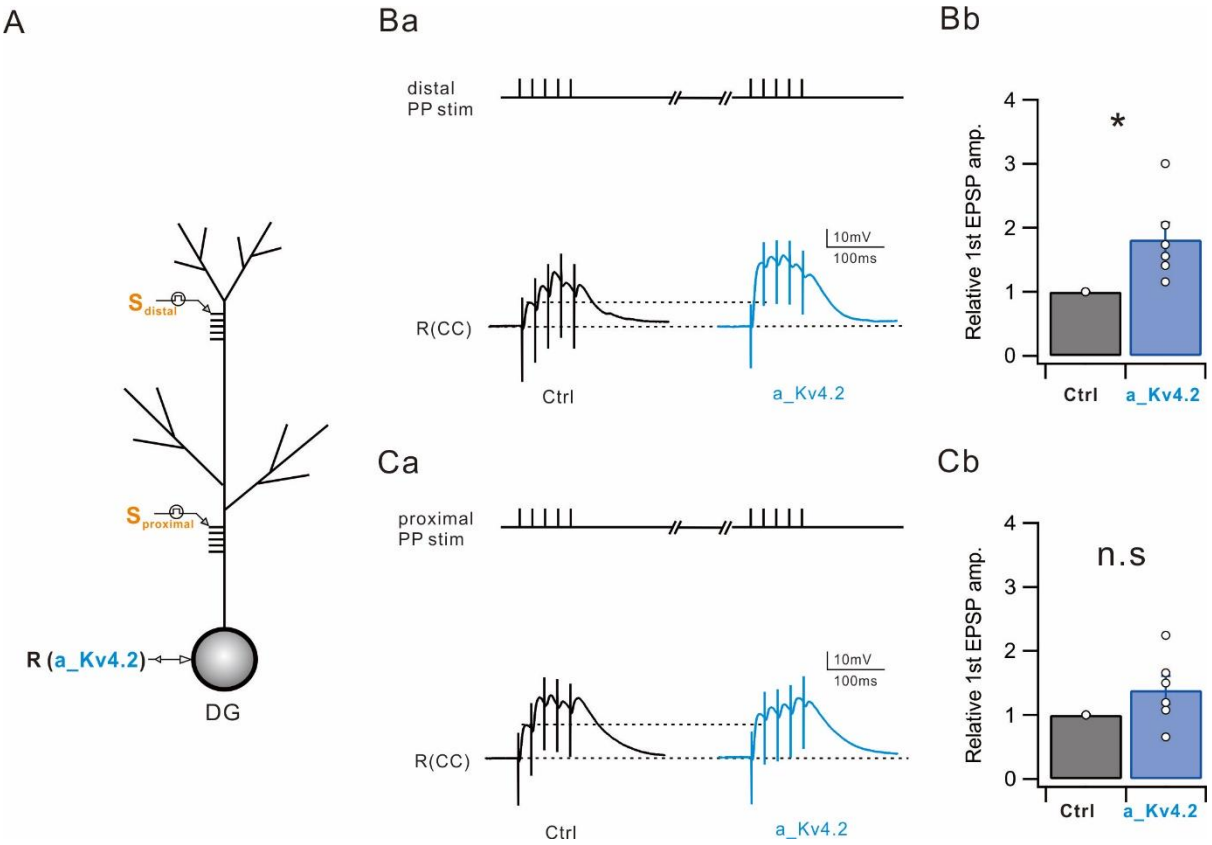

Figure 6. Inhibition of Kv4.2 by anti-Kv4.2 antibody induced increases in EPSP at distal dendrites in DG.

(A) Experimental configurations showing whole-cell recording with stimulation at distal and proximal dendrite in DG.

(Ba) Representative traces of summated EPSP recorded from soma in response to 50 Hz stimulation at distal dendrites before (black) and after (blue) anti-Kv4.2 antibody perfusion.

(Bb) Bar graphs summarize relative amplitude of the 1st EPSP (n = 6) in control (black) and after anti-Kv4.2 antibody perfusion (blue).

(Ca) Representative traces of summated EPSP recorded from soma in response to 50 Hz stimulation at proximal dendrites before (black) and after (blue) anti-Kv4.2 antibody perfusion.

(Cb) Bar graphs summarize relative amplitude of the 1st EPSP (n = 6) in control (black) and after anti-Kv4.2 antibody perfusion (blue).

n.s, $p > 0.05$, *, $p < 0.05$, **, $p < 0.01$. Circles represent data from individual experiments and bars indicate mean ± SEM.

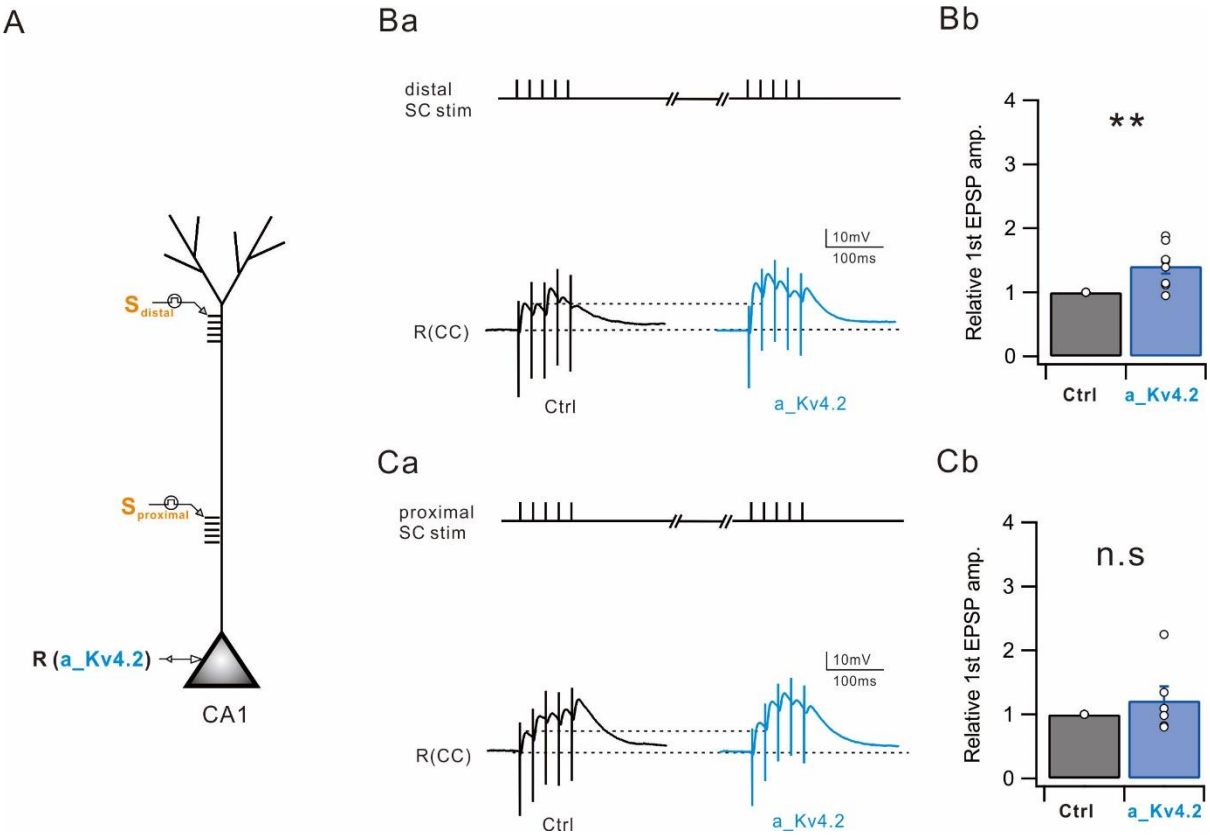

Figure 7. Inhibition of Kv4.2 by anti-Kv4.2 antibody induced increases in EPSP at distal dendrites in CA1.

(A) Experimental configurations showing whole-cell recording with stimulation at distal and proximal dendrite in CA1.

(Ba) Representative traces of summated EPSP recorded from soma in response to 50 Hz stimulation at distal dendrites before (black) and after (blue) anti-Kv4.2 antibody perfusion.

(Bb) Bar graphs summarize relative amplitude of the 1st EPSP (n = 8) in control (black) and after anti-Kv4.2 antibody perfusion (blue).

(Ca) Representative traces of summated EPSP recorded from soma in response to 50 Hz stimulation at proximal dendrites before (black) and after (blue) anti-Kv4.2 antibody perfusion.

(Cb) Bar graphs summarize relative amplitude of the 1st EPSP (n = 6) in control (black) and after anti-Kv4.2 antibody perfusion (blue).

n.s, $p > 0.05$, *, $p < 0.05$, **, $p < 0.01$. Circles represent data from individual experiments and bars indicate mean ± SEM.

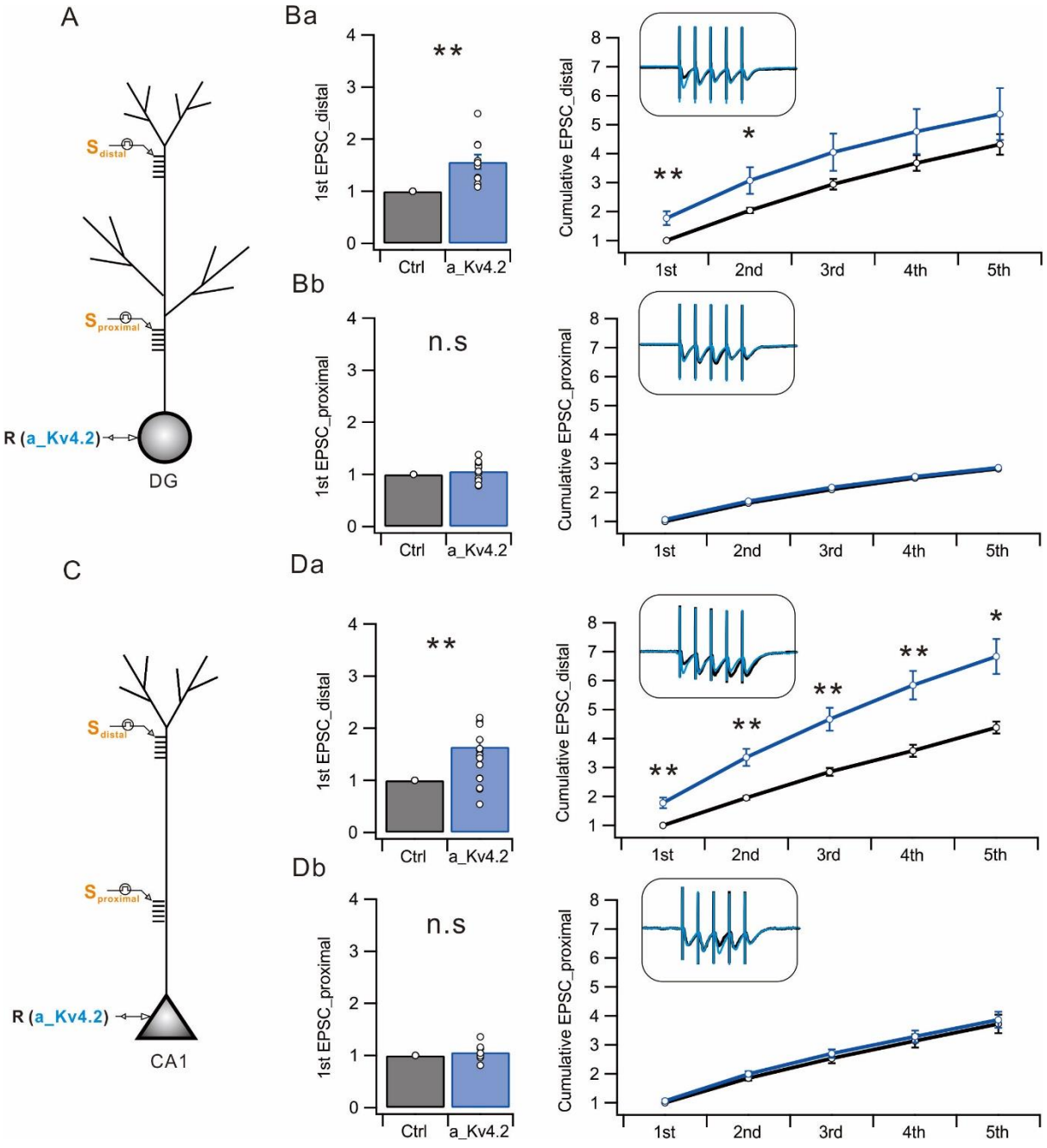

Figure 8. EPSC is potentiated by inhibition of Kv4.2 at distal dendrites, but not at proximal dendrites.

(A) Experimental configurations showing whole-cell recording with stimulation at distal and proximal dendrite in DG.

(Ba) Left, summary data showing an increase in the 1st EPSC amplitude by stimulation at distal dendrites in control (black) and anti-Kv4.2 (blue) (n = 10). Right, averaged cumulative EPSC in response to stimulation.

(Bb) Left, Summary data showing no significant change in the 1st EPSC elicited by stimulation at proximal dendrites in control (black) and anti-Kv4.2 (blue) (n = 9).

(C) Experimental configurations showing whole-cell recording with stimulation at distal and proximal dendrite in CA1.

(Da) Left, summary data showing an increase in the 1st EPSC amplitude by stimulation at distal dendrites in control (black) and anti-Kv4.2 (blue) (n = 10). Right, averaged cumulative EPSC in response to stimulation.

(Db) Left, Summary data showing no significant change in the 1st EPSC elicited by stimulation at proximal dendrites in control (black) and anti-Kv4.2 (blue) (n = 8). Right, averaged cumulative EPSC in response to stimulation.

n.s, $p > 0.05$, *, $p < 0.05$, **, $p < 0.01$. Circles represent data from individual experiments and bars indicate mean ± SEM.

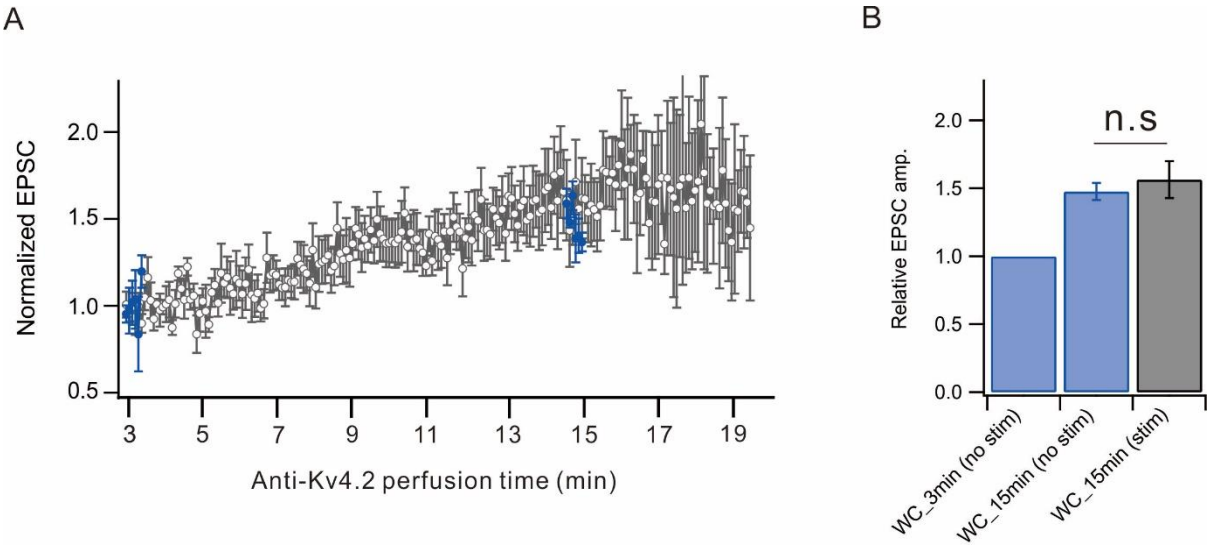

Figure 9. This potentiaion does not depend on synaptic stimulation.

(A) The averaged amplitude obtained during 1 minute for control and 15minutes after patch break-in without any simulation (closed light blue circle).

(B) Bar graphs summarize amplitude of the 1st EPSC in 3 minutes and 15 minutes after patch break-in (n=3).

n.s, $p > 0.05$, *, $p < 0.05$, **, $p < 0.01$. Bars indicate mean ± SEM.

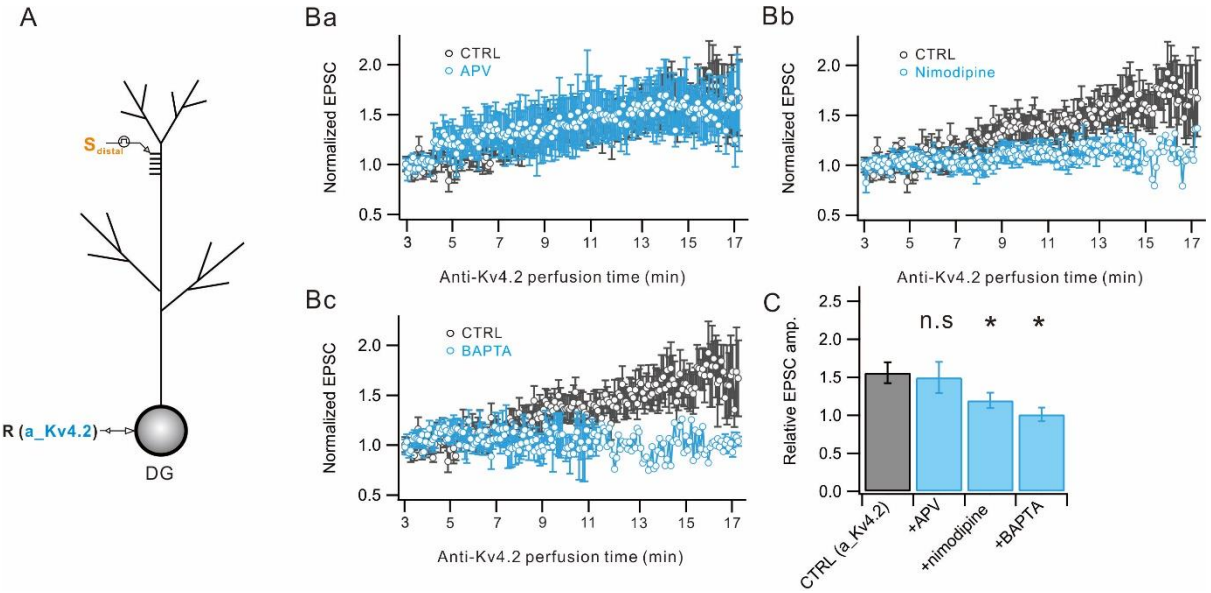

Figure 10. Synaptic potentiation at distal dendrites in DG is mediated by L-type voltage-gated Ca^{2+} channel.

(A) Experimental configuration showing somatic whole-cell clamp recording with stimulation at distal dendritic region in DG.

(Ba) Time course of anti-Kv4.2 antibody effects on EPSC evoked by stimulation at distal dendrites with control and APV (n = 4).

(Bb) Time course of anti-Kv4.2 antibody effects on EPSC evoked by stimulation at distal dendrites with control and nimodipine (n = 8).

(Bc) Time course of anti-Kv4.2 antibody effects on EPSC evoked by stimulation at distal dendrites with control and BAPTA added solution (n = 6).

(C) Bar graphs summarize amplitude of the 1st EPSC in control, APV, nimodipine and BAPTA internal.

n.s, $p > 0.05$, *, $p < 0.05$, **, $p < 0.01$. Bars indicate mean ± SEM.

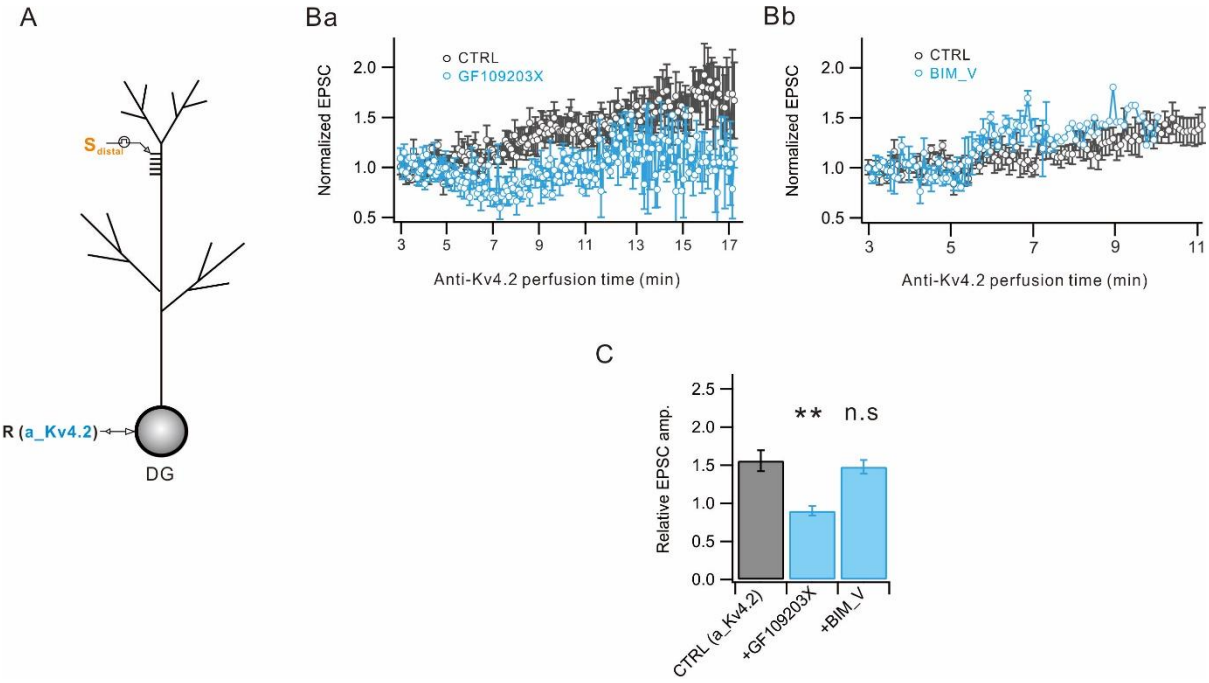

Figure 11. PKC is involved in the novel form of synaptic plasticity.

(A) Experimental configuration showing somatic whole-cell clamp recording with stimulation at distal dendritic region in DG.

(Ba) Time course of anti-Kv4.2 antibody effects on EPSC evoked by stimulation at distal dendrites with control and GF109203X (n = 5).

(Bb) Time course of anti-Kv4.2 antibody effects on EPSC evoked by stimulation at distal dendrites with control and BIM-V (n = 3).

(C) Bar graphs summarize amplitude of the 1st EPSC in control, GF109203X and BIM-V.

n.s, $p > 0.05$, *, $p < 0.05$, **, $p < 0.01$. Bars indicate mean ± SEM.

		DG		CA1	
		Control	w/anti-Kv4.1	Control	w/anti-Kv4.1
EPSP (mV)	distal	16.3 ± 2.4	20.0 ± 2.6	8.3 ± 0.7	9.2 ± 0.9
	proximal	14.0 ± 2.0	19.6 ± 1.9 *	7.1 ± 0.8	7.8 ± 1.0
EPSC (pA)	distal	221.5 ± 16.5	222.9 ± 23.2	150.0 ± 12.0	147.7 ± 5.5
	proximal	238.8 ± 37.9	242.1 ± 53.3	171.0 ± 17.8	156.1 ± 15.2

		DG		CA1	
		Control	w/anti-Kv4.2	Control	w/anti-Kv4.2
EPSP (mV)	distal	15.2 ± 2.4	25.5 ± 3.3*	7.2 ± 1.0	9.4 ± 0.6**
	proximal	15.8 ± 2.6	22.7 ± 3.7	7.0 ± 0.7	8.1 ± 1.2
EPSC (pA)	distal	182.7 ± 27.0	305.2 ± 42.8**	126.6 ± 20.0	198.4 ± 13.4**
	proximal	196.1 ± 21.8	218.6 ± 29.7	124.9 ± 14.0	133.8 ± 16.8

Table 1. The excitatory postsynaptic responses by inhibition of K channels in DG and CA1.

All values are shown as mean ± SEM. Statistical significances were evaluated by Student's t-test, and statistically significant differences were indicated by the number of marks (*, $p < 0.05$; **, $p < 0.01$).

DISCUSSION

K^+ channels show great diversity in the mammalian nervous system. For a decade, subunits of voltage-dependent K^+ channel in neurons have been focused on by neuroscientists explaining neuronal functions to modulate synaptic integration. Among these, the voltage-gated K^+ channel subunit Kv4.2 has evoked much interest. Kv4.2 mediates transient K^+ currents in dendrites of hippocampal CA1 pyramidal neurons (X Chen et al., 2006). In particular, the conventional NMDA receptor-dependent synaptic LTP in hippocampal neurons regulates the distribution of A-type K^+ channels in spines and dendrites, indicating the existence of dynamic functions of these channels in memory mechanisms. Dendritic A-type K^+ current activity, regulating neuronal excitability and associated Ca^{2+} influx, has the potential to impact LTP on many levels (S Watanabe et al., 2002; J Kim et al., 2005; X Chen et al., 2006; J Kim et al., 2007). Previous work from the Johnston group has shown Kv4.2 to be important for the induction of LTP induced by theta-burst pairing (X Chen et al., 2006). However, my finding focused that Kv4.2 expression level affects the degree of synaptic strength and synaptic consequences by Kv4.2 channel inhibition rather than the activity of Kv4.2 channels during LTP induction. My results would further suggest an important role for Kv4.2 channels activation in this type of synaptic plasticity.

There are several studies show that altering Kv4.2 expression levels can lead to altered NMDA receptor-dependent Ca^{2+} signaling and remodeling of NMDA synapses (X Chen et al., 2006). It was reported that Kv4.2 current levels regulate the subunit composition of NMDA receptors, thereby controlling the degree of synaptic strength (SC Jung et al., 2008). Among the Kv4 family with synaptic plasticity, the LTP that accompanied by an effect of Kv4.2 channels is the most widely studied. However, my study clearly showed that synaptic plasticity

associated with Kv4.2 is distinct from a general view of synaptic plasticity.

In my experiment, I observed a novel form of synaptic potentiation driven by inhibition of Kv4.2 in distal dendrites. This potentiation with specific to Kv4.2 is surprisingly accordant with the distribution of Kv4.2 in hippocampal neurons. As shown in overall data, I demonstrated this enhancement in synaptic strength by recording the amplitude of EPSC.

I found out that this potentiation was suppressed when nimodipine applied. More specifically, although the potentiation described in this paper is unlikely to be equivalent to conventional NMDAR-dependent LTP, my results show that increases in synaptic strength predominantly brought by activation of L-type voltage-gated Ca^{2+} channel. Subsequently, I elucidated that potentiation is in association with Ca^{2+} concentrations by using BAPTA internal.

In my final experiments, I elicited that the synaptic potentiation is regulated by PKC activation via the L-type Ca^{2+} channel. By this observation, I can expect that PKC play a pivotal role in intracellular signaling cascades and its mechanisms thought to be involved in synaptic plasticity.

Various intracellular concentrations of calcium play a key role in long-term potentiation (LTP) (CE Jahr and CF Stevens, 1987; GL Westbrook and ML Mayer, 1987). The increased intracellular calcium can be introduced via multiple calcium-conducting channels. The induction of NMDA receptor-dependent LTP requires calcium influx into the postsynaptic region via the activated NMDA receptors. Conventionally, high-frequency stimulation can induce LTP in both DG and CA1 regions. However, it is also possible to induce an LTP which is NMDA receptor-independent by deriving calcium from other sources. One of the sources is voltage-gated calcium channel (LM Grover and TJ Teyler, 1990; H Miyakawa et al., 1992).

Taken together, LTP is mediated by several protein kinases and phosphatases (K Fukunaga,

1993; TR Soderling and VA Derkach, 2000; J Lisman et al., 2002). For example, the phosphorylation activity of calcium / calmodulin-dependent protein kinase II (CaMKII) is enhanced following LTP induction (K Fukunaga et al., 1993; J Liu et al., 1999; K Fukunaga and E Miyamoto, 2000). Likewise CaMKII, PKC activity is essential for the induction of LTP in the hippocampus (GL Collingridge et al., 2004; S Moriguchi et al., 2009).

In contrast to the multiple studies of LTP in DG and CA1, the effect of direct K^+ channel modulation has not been investigated intensively. Until now, no studies have been conducted to compare inhibition of K^+ channel on these two regions in hippocampal slices. In this study, I first conducted a series of experiments in excitatory postsynaptic potential (EPSP) recorded from DG and CA1. Differential effects of K^+ channel in the two regions were investigated. My results demonstrate that the synaptic potentiation by Kv4.2 inhibition occurs both DG and CA1 via NMDA receptor-independent mechanisms. The L-type voltage-gated Ca^{2+} channel is the main mediator for the NMDA receptor-independent potentiation. For Kv4.1, by contrast, I could not observe this synaptic plasticity.

The major finding of this series of studies is that Kv4.1 / 4.2 differentially affects synaptic plasticity in the DG and CA1. The distinct density of Kv4.2 could account for the differential effect of Kv4.2 in proximal and distal dendrites. It has been reported that Kv4.2 is much more abundant in distal dendrites than in soma and proximal dendrites. Thus, the different response could be considered as a consequence of the distinct density and distribution of Kv4.2 channels in DG and CA1. On the other hand, for Kv4.1, it is revealed to high density in somatic and proximal dendrite in DG granule cells, whereas they were shown in low density in CA1. This evidence may account for why the effect is much smaller in CA1.

Here I found that Kv4.2 inhibition stimulates PKC activities, thereby leading to potentiation of NMDA receptor-independent potentiation. The PKC activation was required for

this form of potentiation by Kv4.2 channel inhibition. Thus channel modulation with activation of PKC underlies the enhancement of synaptic plasticity, thereby improving the cognitive and learning in the hippocampus.

REFERENCES

Aniksztejn, L., and Y. Ben-Ari. 1991. Novel form of long-term potentiation produced by a K+ channel blocker in the hippocampus. *Nature*. 349:67-69.

Baldwin, T.J., M.L. Tsaur, G.A. Lopez, Y.N. Jan, and L.Y. Jan. 1991. Characterization of a mammalian cDNA for an inactivating voltage-sensitive K+ channel. *Neuron*. 7:471-483.

Baron, A., G. Loirand, P. Pacaud, C. Mironneau, and J. Mironneau. 1993. Dual effect of thrombin on voltage-dependent Ca2+ channels of portal vein smooth muscle cells. *Circ. Res.* 72:1317-1325.

Bear, M.F., and R.C. Malenka. 1994. Synaptic plasticity: LTP and LTD. *Curr. Opin. Neurobiol.* 4:389-399.

Birnbaum, S.G., A.W. Varga, L.L. Yuan, A.E. Anderson, J.D. Sweatt, and L.A. Schrader. 2004. Structure and function of Kv4-family transient potassium channels. *Physiol. Rev.* 84:803-833.

Bliss, T.V., and G.L. Collingridge. 1993. A synaptic model of memory: long-term potentiation in the hippocampus. *Nature*. 361:31-39.

Chen, X., L.L. Yuan, C. Zhao, S.G. Birnbaum, A. Frick, W.E. Jung, T.L. Schwarz, J.D. Sweatt, and D. Johnston. 2006. Deletion of Kv4.2 gene eliminates dendritic A-type K+ current and enhances induction of long-term potentiation in hippocampal CA1 pyramidal neurons. *J. Neurosci.* 26:12143-12151.

Collingridge, G.L., J.T. Isaac, and Y.T. Wang. 2004. Receptor trafficking and synaptic plasticity. *Nat. Rev. Neurosci.* 5:952-962.

Collingridge, G.L., S. Peineau, J.G. Howland, and Y.T. Wang. 2010. Long-term depression in the CNS. *Nat. Rev. Neurosci.* 11:459-473.

Coogan, A.N., D.M. O'Leary, and J.J. O'Connor. 1999. P42/44 MAP kinase inhibitor PD98059 attenuates multiple forms of synaptic plasticity in rat dentate gyrus in vitro. *J. Neurophysiol.* 81:103-110.

Fukunaga, K. 1993. [The role of Ca2+/calmodulin-dependent protein kinase II in the cellular signal transduction]. *Nihon Yakurigaku Zasshi*. 102:355-369.

Fukunaga, K., and E. Miyamoto. 2000. A working model of CaM kinase II activity in hippocampal long-term potentiation and memory. *Neurosci. Res.* 38:3-17.

Fukunaga, K., L. Stoppini, E. Miyamoto, and D. Muller. 1993. Long-term potentiation is associated with an increased activity of Ca2+/calmodulin-dependent protein kinase II. *J. Biol. Chem.* 268:7863-7867.

Grover, L.M., and T.J. Teyler. 1990. Two components of long-term potentiation induced by different patterns of afferent activation. *Nature*. 347:477-479.

Hanse, E., and B. Gustafsson. 1994. TEA elicits two distinct potentiations of synaptic transmission in the CA1 region of the hippocampal slice. *J. Neurosci.* 14:5028-5034.

Hoffman, D.A., J.C. Magee, C.M. Colbert, and D. Johnston. 1997. K+ channel regulation of signal propagation in dendrites of hippocampal pyramidal neurons. *Nature*. 387:869-875.

Huang, Y.Y., and R.C. Malenka. 1993. Examination of TEA-induced synaptic enhancement in area CA1 of the hippocampus: the role of voltage-dependent Ca2+ channels in the induction of LTP. *J. Neurosci.* 13:568-576.

Jahr, C.E., and C.F. Stevens. 1987. Glutamate activates multiple single channel conductances in hippocampal neurons. *Nature*. 325:522-525.

Johnston, J., I.D. Forsythe, and C. Kopp-Scheinpflug. 2010. Going native: voltage-gated potassium channels controlling neuronal excitability. *J. Physiol.* 588:3187-3200.

Jung, S.C., J. Kim, and D.A. Hoffman. 2008. Rapid, bidirectional remodeling of synaptic NMDA receptor subunit composition by A-type K+ channel activity in hippocampal CA1 pyramidal neurons. *Neuron*. 60:657-671.

Kerti, K., A. Lorincz, and Z. Nusser. 2012. Unique somato-dendritic distribution pattern of Kv4.2 channels on hippocampal CA1 pyramidal cells. *Eur. J. Neurosci.* 35:66-75.

Khaliq, Z.M., and B.P. Bean. 2008. Dynamic, nonlinear feedback regulation of slow pacemaking by A-type potassium current in ventral tegmental area neurons. *J. Neurosci.* 28:10905-10917.

Kim, J., and D.A. Hoffman. 2008. Potassium channels: newly found players in synaptic plasticity. *Neuroscientist*. 14:276-286.

Kim, J., S.C. Jung, A.M. Clemens, R.S. Petralia, and D.A. Hoffman. 2007. Regulation of dendritic excitability by activity-dependent trafficking of the A-type K+ channel subunit Kv4.2 in hippocampal neurons. *Neuron*. 54:933-947.

Kim, J., D.S. Wei, and D.A. Hoffman. 2005. Kv4 potassium channel subunits control action potential repolarization and frequency-dependent broadening in rat hippocampal CA1 pyramidal neurones. *J. Physiol.* 569:41-57.

Kole, M.H., J.J. Letzkus, and G.J. Stuart. 2007. Axon initial segment Kv1 channels control axonal action potential waveform and synaptic efficacy. *Neuron*. 55:633-647.

Lien, C.C., and P. Jonas. 2003. Kv3 potassium conductance is necessary and kinetically optimized for high-frequency action potential generation in hippocampal interneurons. *J. Neurosci.* 23:2058-2068.

Lisman, J., H. Schulman, and H. Cline. 2002. The molecular basis of CaMKII function in synaptic and behavioural memory. *Nat. Rev. Neurosci.* 3:175-190.

Liss, B., O. Franz, S. Sewing, R. Bruns, H. Neuhoff, and J. Roeper. 2001. Tuning pacemaker frequency of individual dopaminergic neurons by Kv4.3L and KChip3.1 transcription. *EMBO J.* 20:5715-5724.

Liu, J., K. Fukunaga, H. Yamamoto, K. Nishi, and E. Miyamoto. 1999. Differential roles of Ca(2+)/calmodulin-dependent protein kinase II and mitogen-activated protein kinase activation in hippocampal long-term potentiation. *J. Neurosci.* 19:8292-8299.

Long, S.B., E.B. Campbell, and R. Mackinnon. 2005. Crystal structure of a mammalian voltage-dependent Shaker family K+ channel. *Science*. 309:897-903.

Malenka, R.C., and R.A. Nicoll. 1999. Long-term potentiation--a decade of progress? *Science*. 285:1870-1874.

Martina, M., J.H. Schultz, H. Ehmke, H. Monyer, and P. Jonas. 1998. Functional and molecular differences between voltage-gated K+ channels of fast-spiking interneurons and pyramidal neurons of rat hippocampus. *J. Neurosci.* 18:8111-8125.

Miyakawa, H., W.N. Ross, D. Jaffe, J.C. Callaway, N. Lasser-Ross, J.E. Lisman, and D. Johnston. 1992. Synaptically activated increases in Ca2+ concentration in hippocampal CA1 pyramidal cells are primarily due to voltage-gated Ca2+ channels. *Neuron*. 9:1163-1173.

Moriguchi, S., N. Shioda, F. Han, J.Z. Yeh, T. Narahashi, and K. Fukunaga. 2009. Galantamine enhancement of long-term potentiation is mediated by calcium/calmodulin-dependent protein kinase II and protein kinase C activation. *Hippocampus*. 19:844-854.

Murakoshi, H., and J.S. Trimmer. 1999. Identification of the Kv2.1 K+ channel as a major component of the delayed rectifier K+ current in rat hippocampal neurons. *J. Neurosci.* 19:1728-1735.

Onuma, H., Y.F. Lu, K. Tomizawa, A. Moriwaki, M. Tokuda, O. Hatase, and H. Matsui. 1998. A calcineurin inhibitor, FK506, blocks voltage-gated calcium channel-dependent LTP in the hippocampus. *Neurosci. Res.* 30:313-319.

Pak, M.D., K. Baker, M. Covarrubias, A. Butler, A. Ratcliffe, and L. Salkoff. 1991. mShal, a subfamily of A-type K+ channel cloned from mammalian brain. *Proc. Natl. Acad. Sci. U. S. A.* 88:4386-4390.

Pongs, O. 2008. Regulation of excitability by potassium channels. *In* Results Probl. Cell Differ. Vol. 44. 145-161.

Ramakers, G.M., P. Pasinelli, M. van Beest, A. van der Slot, W.H. Gispen, and P.N. De Graan. 2000. Activation of pre- and postsynaptic protein kinase C during tetraethylammonium-induced long-term potentiation in the CA1 field of the hippocampus. *Neurosci. Lett.* 286:53-56.

Serodio, P., and B. Rudy. 1998. Differential expression of Kv4 K+ channel subunits mediating subthreshold transient K+ (A-type) currents in rat brain. *J. Neurophysiol.* 79:1081-1091.

Serodio, P., E. Vega-Saenz de Miera, and B. Rudy. 1996. Cloning of a novel component of A-type K+ channels operating at subthreshold potentials with unique expression in heart and brain. *J. Neurophysiol.* 75:2174-2179.

Soderling, T.R., and V.A. Derkach. 2000. Postsynaptic protein phosphorylation and LTP. *Trends Neurosci.* 23:75-80.

Ster, J., F. de Bock, F. Bertaso, K. Abitbol, H. Daniel, J. Bockaert, and L. Fagni. 2009. Epac mediates PACAP-dependent long-term depression in the hippocampus. *J. Physiol.* 587:101-113.

Toullec, D., P. Pianetti, H. Coste, P. Bellevergue, T. Grand-Perret, M. Ajakane, V. Baudet, P. Boissin, E. Boursier, F. Loriolle, and et al. 1991. The bisindolylmaleimide GF 109203X is a potent and selective inhibitor of protein kinase C. *J. Biol. Chem.* 266:15771-15781.

Watanabe, S., D.A. Hoffman, M. Migliore, and D. Johnston. 2002. Dendritic K+ channels contribute to spike-timing dependent long-term potentiation in hippocampal pyramidal neurons. *Proc. Natl. Acad. Sci. U. S. A.* 99:8366-8371.

Westbrook, G.L., and M.L. Mayer. 1987. Micromolar concentrations of Zn2+ antagonize NMDA and GABA responses of hippocampal neurons. *Nature*. 328:640-643.

Zhuo, M., and R.D. Hawkins. 1995. Long-term depression: a learning-related type of synaptic plasticity in the mammalian central nervous system. *Rev. Neurosci.* 6:259-277.

ABSTRACT IN KOREAN

A-type K^+ channel 은 임계 이하의 시냅스 전위의 통합에 중요하며, A-type K^+ channel 의 조절에 의한 신호 전달 기작이 신경 흥분성에 중대한 영향을 미칠 수 있다고 제안된다. Kv4 계열 중에서 Kv4.1 과 Kv4.2 채널의 고유 특성이 널리 연구되고 있다. 그러나 오늘날까지 시냅스 가소성에서 A-type K^+ channel 의 기여는 알려지지 않았다.

시냅스 변형에 대한 K^+ channel 의 억제 효과를 DG 및 CA1에서 비교하였다. Perforant path-DG granule cell 또는 Schaffer collateral-CA1 pyramidal cell 에 50 Hz 자극을 가하였다. Kv4.1 / Kv4.2 에 항체를 이용하여 시냅스 반응을 관찰하고 Kv4.2 channel 이 시냅스 가소성과 상관 관계가 있음을 발견하였다. 나의 데이터는 Kv4.2 의 억제가 시냅스 가소성의 증강을 유도하는 반면, Kv4.1 항체는 영향을 미치지 않는다는 것을 입증하였다. 이 가소성 형태는 이전에 연구되었던 일반적인 장기 가소성과는 다른 형태이다.

시냅스 가소성에 영향을 미치는 메커니즘을 조사하였다. NMDA 수용체 차단제인 APV가 부분적으로 DG 에서의 강화 작용을 차단한다는 것이 관찰되었다. 그러나, nimodipine (L-type voltage-gated Ca2 + channel 길항제) 이 가해질 때 강화 작용의 완전한 차단이 일어났다. 또한 PKC는 세포 내 신호 전달 계통과 시냅스 가소성에 관여하는 것으로 생각되는 메커니즘에 중요한 역할을 함을 알았다. 나의 결과는 해마의 DG 와 CA1 에서 Kv4.1 / Kv4.2 에 대해 뚜렷이 구분되는 밀도와 분포의 증거를 뒷받침한다. 또한, 이 연구에서, 나는 이러한 시냅스 가소성이 일반적인 시냅스 가소성 및 그 메커니즘과는 다른 Kv4.2 와 관련된 가소성

임을 분명히 보여준다.

중심 단어 : **A-type K^+ current, Kv4.1, Kv4.2,** 시냅스 가소성, 장기 강화 작용 **(LTP), DG granule cells, CA1 pyramidal cells**

학 번 : 2015-22026